Solvent Effects on ATRP of Oligo(ethylene glycol) Methacrylate. Exploring the Limits of Control

Helena Bergenudd,*,† Geraldine Coullerez,†,‡ Mats Jonsson,† and Eva Malmström§

Nuclear Chemistry, KTH Chemical Science and Engineering, Royal Institute of Technology, SE-100 44 Stockholm, Sweden, and Fibre and Polymer Technology, KTH Chemical Science and Engineering, Royal Institute of Technology, SE-100 44 Stockholm, Sweden

Received December 22, 2008; Revised Manuscript Received March 12, 2009

ABSTRACT: Five copper complexes in combination with six monomer−solvent mixtures have been used to investigate the solvent effects on ATRP of oligo(ethylene glycol) methacrylate (OEGMA). The redox properties of the copper complexes in OEGMA−solvent mixtures and the apparent rate constants (k_p^{app}) for ATRP of OEGMA were correlated to the degree of control over the polymerizations. Based on this correlation, a general discussion of the limits of control in ATRP is carried out. One of the key parameters for control in ATRP is the propagation rate constant, making the choice of monomer essential for the design of an ATRP system. Also, the solvent effects on the ATRP equilibrium constant (K_{ATRP}) affect the limit of control (i.e., the apparent rate constant above which control is lost). The choice of copper complex is also more important than the choice of solvent for the design of a well-controlled ATRP system.

Introduction

Atom transfer radical polymerization (ATRP)[1,2] is one of the most effective methods for controlled/"living" polymerization. By minimizing the radical concentration through the dynamic equilibrium in Scheme 1, which is mediated by a transition metal complex, and thereby suppressing termination reactions, control over the molecular weight and polymer architecture is enabled.

The equilibrium constant ($K_{ATRP} = k_{act}/k_{deact}$), and hence the control over the polymerization reaction, is largely governed by the properties of the transition metal complex. The most commonly used transition metal so far has been copper in combination with various complexing ligands, including nitrogen-based ligands such as PMDETA,[3] 2,2′-bipyridine[4] and Me_6-TREN.[5] The complexing ligands help solubilizing the transition metal ion and thereby affect the reduction potential of the metal ion. It has previously been shown that the redox properties of the transition metal complex is one of the parameters governing the ATRP equilibrium.[6−8] Coullerez et al.[9] investigated the redox properties of a number of copper complexes in different solvents. The redox properties were found to be significantly affected by the solvent. Furthermore, the solvent effect on the potential appears to be higher for complexes having higher degrees of freedom, compared to complexes with more rigid structures (having lower degrees of freedom).

ATRP has been performed in a wide range of solvents, from nonpolar solvents such as xylene[10] and toluene[11] to polar solvents such as 2-propanol[12] and water.[13,14] Whereas good control is usually achieved in bulk and nonpolar solvents, the use of polar solvents, and in particular water, often leads to limited control over the polymerization.[15−18]

Systematic investigations of solvent effects on the polymerization performance/control (i.e., kinetics and polymer properties) in ATRP are few. Studies on the effect of solvent polarity on activation and deactivation rate constants have shown that the activation rate constant (k_{act}) increases with increasing solvent polarity,[19−21] whereas the deactivation rate constant (k_{deact}) decreases with increasing solvent polarity.[21] This is in agreement with observations of faster and less controlled polymerizations in more polar solvents. However, in recent studies, with a wider range of solvents, the effect of solvent polarity on k_{act}[22] and on K_{ATRP}[23] was less obvious.

A correlation was previously found[8] between the apparent rate constant (k_p^{app}) for ATRP of oligo(ethylene glycol) methacrylate (OEGMA) in water and the redox properties of the copper complexes measured in OEGMA−water mixtures. A similar correlation was found for the equilibrium constant (K_{ATRP}) in MeCN.[7] It was also found in the work by Coullerez et al.[8] that potentials measured in pure water were not correlated to the potentials in OEGMA−water mixtures. However, the degree of control over the polymerization was not investigated.

In this work, the studies of the solvent effects on ATRP by Coullerez et al.[8,9] have been extended to OEGMA−solvent mixtures, including the OEGMA−water mixture from ref 8. The investigation of the correlation between the redox properties of a number of copper complexes and the apparent rate constants (k_p^{app}) for ATRP of OEGMA is related to the degree of control over the polymerization. On the basis of the log(k_p^{app}) vs potential plots and the characteristics (i.e., molecular weights and molecular weight distribution) of the synthesized polymers, a general discussion of the limits of control in ATRP is carried out.

Experimental Section

Materials. Monomethoxy-capped oligo(ethylene glycol) methacrylate (OEGMA) with an average molecular weight of 475 g/mol was obtained from Aldrich. For the polymerizations, the inhibitors were

Scheme 1. Mechanism for ATRP

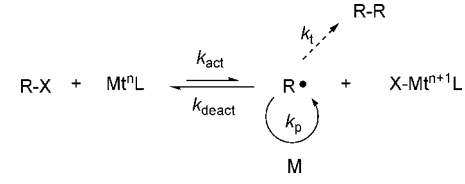

* Corresponding Author: E-mail: hebe@kth.se; Phone: +46 8 790 9279; Fax: +46 8 790 8772.
† Nuclear Chemistry, KTH Chemical Science and Engineering, Royal Institute of Technology.
‡ Present address: Laboratory for Surface Science and Technology, Swiss Federal Institute of Technology, Wolfgang-Pauli-Strsse 10, 8093 Zürich, Switzerland.
§ Fibre and Polymer Technology, KTH Chemical Science and Engineering, Royal Institute of Technology.

10.1021/ma8028425 CCC: $40.75
Published on Web 04/16/2009

removed by passing OEGMA through a column of neutral aluminum oxide. The oligo(ethylene glycol)-based initiator (OEGBr) was synthesized from monomethoxy-capped oligo(ethylene glycol) (Aldrich, mean degree of polymerization 7−8) and 2-bromoisobutyryl bromide (98%) using a modification of a literature procedure,[24] purifying the crude product after extraction by flash chromatography, eluting the product in 30/70 methanol/ethyl acetate. Silica gel (40−63 μm) for flash chromatography was obtained from VWR. The ligand tris[2-(dimethylamino)ethyl]amine (Me_6-TREN) was synthesized according to literature procedure.[25] The other ligands were purchased from Aldrich and used as received, i.e. 2,2′-bipyridine (bipy) (99+%), *N*,*N*,*N*′,*N*″,*N*″-pentamethyldiethylenetriamine (PMDETA) (99%), 1,1,4,7,10,10-hexamethyltriethylenetetraamine (HMTETA) (97%), and 1,4,8,11-tetraaza-1,4,8,11-tetramethylcyclotetradecan (Me_4-cyclam) (98%). CuBr (98%, Aldrich) was used as received for voltammetry measurements, but purified for polymerization experiments: CuBr was stirred in glacial acetic acid, filtered, washed with absolute ethanol and diethyl ether, and dried in vacuum. Deionized Milli-Q water was used. All other chemicals were purchased from conventional suppliers and used as received.

Cyclic Voltammetry. Cyclic voltammetry was performed with a PAR 263A potentiostat/galvanostat interfaced to a base PC using the EG&G Model 270 software package. The cell was a standard three-electrode setup using a 2 mm diameter glassy carbon working electrode, a platinum coil counter electrode and a calomel reference electrode. The scan rate was 200 mV/s and full IR compensation was employed in all measurements. The supporting electrolyte was 0.5 M KCl in water and OEGMA−water and 0.1 M tetrabutylammonium tetrafluoroborate in the other solvents and OEGMA−solvent mixtures. The CV-measurements were conducted in solvent mixtures identical to the ones used in the polymerizations, OEGMA/solvent = 2:1 by weight ([OEGMA]/[CuBr] = 100/1). The potentials were measured using a saturated calomel electrode (SCE) as reference electrode and the voltammograms were reproducible on several scans. Most of the redox processes were quasireversible as seen by the peak-to-peak separation ΔE values ($E_{red} - E_{ox}$) being larger than the ideal 60 mV for a one-electron-transfer process (see Supporting Information).[26] The potentials were measured against ferrocene, a reference redox couple for which the solvent sensitivity is assumed to be very small (ferrocyanide was used in pure water). Three scans were performed for each copper complex/solvent mixture combination.

Polymerizations

Homopolymerization of OEGMA. The polymerizations were performed in OEGMA−solvent mixtures 2:1 by weight. [OEGMA]/[OEGBr]/[CuBr] = 100/1/1 and the Cu/ligand ratio was 1:1.1 for all ligands except for the bipyridine complex where the ratio was 1:2. In a typical polymerization experiment, monomer, solvent and ligand were charged into a dry round-bottomed flask equipped with a magnetic stirring bar, placed on an ice-bath. The flask was sealed and the solution was degassed by purging with argon for 15 min, where after CuBr was added and the resulting solution was degassed for another 15 min. The initiator was mixed separately with a small amount of the monomer and solvent and the resulting solution was degassed with argon for 15 min. To start the polymerization, the initiator solution was added to the monomer solution, placed in an oil-bath at room temperature. Aliquots were withdrawn from the flask at timed intervals to monitor the progress of the polymerization. The monomer conversion was followed by ^{1}H NMR spectroscopy in D_2O and the polymer molecular weight was measured by size exclusion chromatography (SEC) on the withdrawn sample without further purification. The catalyst was removed from the product by passing the polymer solution through a column with neutral aluminum oxide.

Block Copolymers. The previously synthesized poly(OEGMA) was used as macroinitiator for chain extension with OEGMA. The crude product (i.e., poly(OEGMA), remaining monomer and solvent) was charged into a round-bottomed flask together with ligand, solvent (the same as in the crude product) and fresh monomer ([OEGMA]/[macroinitiator]/[CuBr] = 100/1/1; solvent/monomer = 1:2 by weight). The flask was sealed and, while kept on an ice-bath, the solution was degassed by successive vacuum and purging with argon during a total of 30 min. CuBr was added and the solution was allowed to warm to ambient temperature. The product was analyzed by ^{1}H NMR for conversion and SEC for molecular weight.

Analyses

^{1}H NMR Spectroscopy. ^{1}H NMR spectra were recorded on a Bruker Avance 400 MHz NMR instrument using D_2O. Monomer conversion was followed by comparing the disappearing monomer vinyl signals at 5.7 and 6.2 ppm with the growing polymer signal appearing at 4.2 ppm.

Size Exclusion Chromatography (SEC). SEC was performed using a Waters 717 Plus autosampler and a Waters model M-6000A solvent pump equipped with a PL-EMD 960 light scattering evaporative detector, two PLgel 10-mm mixed B columns (300 × 7.5 mm) from Polymer Laboratories, and one Ultrahydrogel linear column (300 × 7.8 mm) from Waters, connected to an IBM-compatible computer. The eluent was *N*,*N*-dimethylformamide (LabScan, Sweden) at a flow rate of 1.0 mL/min and narrow molecular weight linear poly(ethylene oxide) standards were used for calibration. Millennium software version 3.20 was used to process the data.

Results and Discussion

Polymerizations of oligo(ethylene glycol) methacrylate (OEGMA) at room temperature and cyclic voltammetry measurements were performed in OEGMA−solvent mixtures. As it was important to have the same conditions in the electrochemical studies and the polymerizations in order to evaluate the relationship between the kinetics and the redox properties of the copper complexes, the OEGMA−solvent mixtures were identical in the two sets of experiments. Six different solvents, i.e. water, methanol (MeOH), acetonitrile (MeCN), isopropanol (2-PrOH), dimethyl sulfoxide (DMSO), and *N*,*N*-dimethylformamide (DMF), were used in combination with five copper complexes, i.e., CuBr with bipy, PMDETA, HMTETA, Me_6-TREN, and Me_4-cyclam, respectively. Only a selection of solvent-ligand combinations, that is water, DMSO, 2-PrOH, and MeCN with Me_6-TREN, PMDETA, and bipy, were chosen for molecular weight measurements, covering a representative range of rate constants and redox properties.

Redox Properties of the Copper Complexes. The half-wave potentials ($E_{1/2}$) for the copper complexes in pure solvents[9] and in OEGMA−solvent mixtures are shown in Table 1. (Peak-to-peak separation ΔE_p values ($E_{red} - E_{ox}$) are found in Supporting Information.) The general trend in reducing properties for the different copper complexes is the same in all OEGMA−solvent mixtures, i.e. Me_6-TREN > PMDETA > HMTETA > Me_4-cyclam > bipy (e.g., in MeCN, ΔE (Me_6-TREN → bipy) = 370 mV), with the exception of Me_6-TREN in OEGMA−water and in pure water, which have the lowest reducing power of all complexes.

In Figure 1, the potentials for the copper complexes in OEGMA−solvent mixtures (E_{mix}) are plotted against the potentials in pure solvents (E_{pure}). The 1:1 relationship between E_{mix} and E_{pure} is indicated by a straight line. (For comparison, the corresponding figure with the different complexes in the legend is found in the Supporting Information.) The linear trend shows that the potentials in the solvent mixtures are roughly proportional to those in pure solvents. The difference between

Table 1. Half-Wave Potentials[a] (mV vs Ferrocene) for CuBr Complexes in pure Solvents (E_{pure})[9] and OEGMA−Solvent Mixtures (E_{mix}), and Apparent Rate Constants[b] (k_p^{app}, 10^{-3} s^{-1}) for ATRP of OEGMA in OEGMA−Solvent Mixtures at Ambient Temperature

	bipy			Me_4-cyclam			HMTETA		
	E_{pure}	E_{mix}	k_p^{app}	E_{pure}	E_{mix}	k_p^{app}	E_{pure}	E_{mix}	k_p^{app}
2-PrOH	−342	−387	0.03	−364		1.47	−403	−461	0.36
DMF	−381	−371	0.07	−374		1.26	−491	−556	0.34
DMSO	−421	−363	0.25	−431	−396	1.71	−564	−499	1.40
MeOH	−291	−376	0.06	−306	−425	1.31	−286	−383	0.35
MeCN	−421	−429	0.04	−340	−426	0.88	−487	−518	0.14
BuOH	−355	−404		−389			−379	−485	
H_2O[c]	−398[d]	−364	3.42	−251[d]	−443	10.7	−424[d]	−486	6.12

	PMDETA			Me_6-TREN		
	E_{pure}	E_{mix}	k_p^{app}	E_{pure}	E_{mix}	k_p^{app}
2-PrOH	−477	−509	0.32	−809	−778	0.55
DMF	−642	−615	0.49	−764	−808	0.95
DMSO	−690	−617	2.14	−787	−735	1.89
MeOH	−527	−552	0.97	−719	−752	0.45
MeCN	−489	−675	0.58	−717	−796	0.90
BuOH	−492	−538		−794		
H_2O[c]	−325[d]	−568	4.21	−91[d]	−288	2.39

[a] The average values from three CV scans. [b] Average values from 2−3 polymerizations, values given ± 36%. [c] Supporting electrolyte in water and in OEGMA−water mixtures is KCl. [d] mV vs ferrocyanide, these values are not included in ref 9.

the potentials in pure solvent and in the mixture is not large for any of the solvents or complexes. The potentials measured in water and OEGMA−water mixtures are more scattered and deviate significantly from the 1:1 relationship. The reason for this can be more specific solvation of amines in water, due to protonation, that does not take place in the other solvents. The magnitude of the solvent effects, measured as the difference between the highest and the lowest potential for a particular copper complex, decreases going from the pure solvents to the OEGMA−solvent mixtures (not including the OEGMA−water mixture), e.g., for HMTETA, $\Delta E_{pure} = E_{MeOH} - E_{DMSO} = 278$ mV and $\Delta E_{mix} = E_{MeOH} - E_{DMF} = 173$ mV; and for Me_6-TREN, $\Delta E_{pure} = E_{MeCN} - E_{2\text{-PrOH}} = 92$ mV and $\Delta E_{mix} = E_{DMSO} - E_{DMF} = 73$ mV. The rationale for this is that OEGMA constitutes the major part of the solvent mixture and solvation is therefore largely governed by the properties of OEGMA.

The solvent effects on the redox properties were analyzed in terms of Kamlet−Taft relationships, see Supporting Information. The solvent independent coefficients were calculated for the potentials. However, too few solvents have been included in this study to allow a quantitative evaluation of the coefficients. Plotting the estimated potentials, using the Kamlet−Taft relationships, against the experimental potentials, gives a good fit ($R^2 = 1.00$, Supporting Information; comparable to ref 9). The OEGMA−water mixtures were not included in the analyzes, due to the special properties of water (in particular the large value of the Hildebrand parameter, δ_H) which distorts the data set. The relative importance of the different solvent properties must be evaluated to extract physicochemical information from the Kamlet−Taft relationships. This can be extracted from the so-called beta coefficients. The relative importance of the Kamlet−Taft parameters for the potentials is summarized in Table S5 (Supporting Information). There is a shift in the relative importance of the parameters between pure solvents and OEGMA−solvent mixtures. Though OEGMA is the dominating part of the solvent mixture, it is obvious that the added solvent affects the redox properties significantly. The ligands are also affected differently by the solvent properties, although there is no single parameter that dominates for any of the ligands.

Correlation between Redox Properties and Kinetics. The initial slopes in the plots of $\ln([M]_0/[M])$ vs time (Supporting Information) gives the apparent rate constants (k_p^{app}) for the polymerizations (Table 1). The logarithm of k_p^{app} was plotted against the half-wave potentials in the different OEGMA−solvent mixtures (E_{mix}), Figure 2, where also the average (i.e., average $\log(k_p^{app})$ vs average E_{mix}) for each complex is shown. (For comparison, the corresponding figure with the different complexes in the legend is found in Supporting Information.)

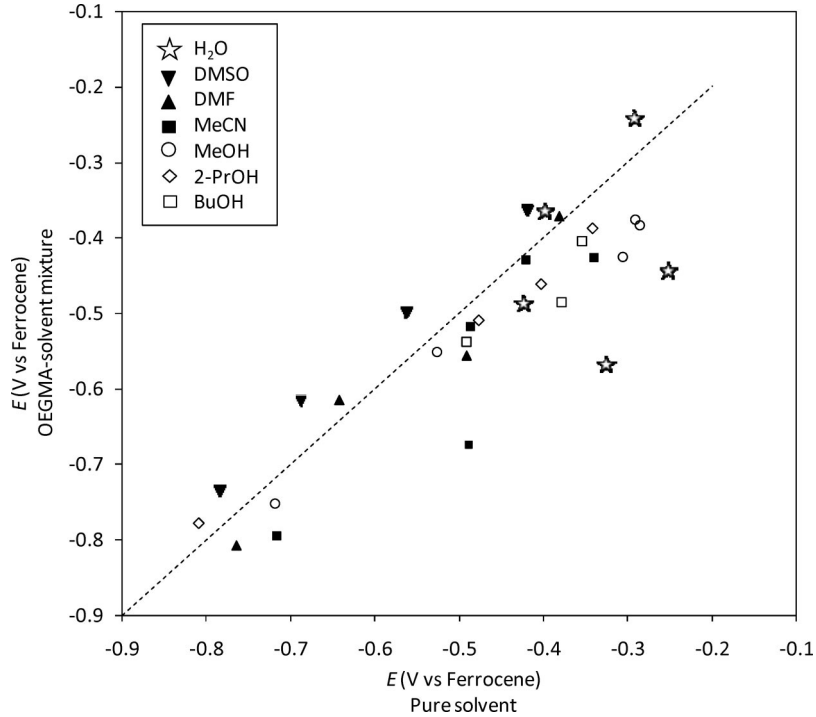

Figure 1. Half-wave potentials for various copper complexes in pure solvents and in OEGMA−solvent mixtures. Dotted line = 1:1 relationship.

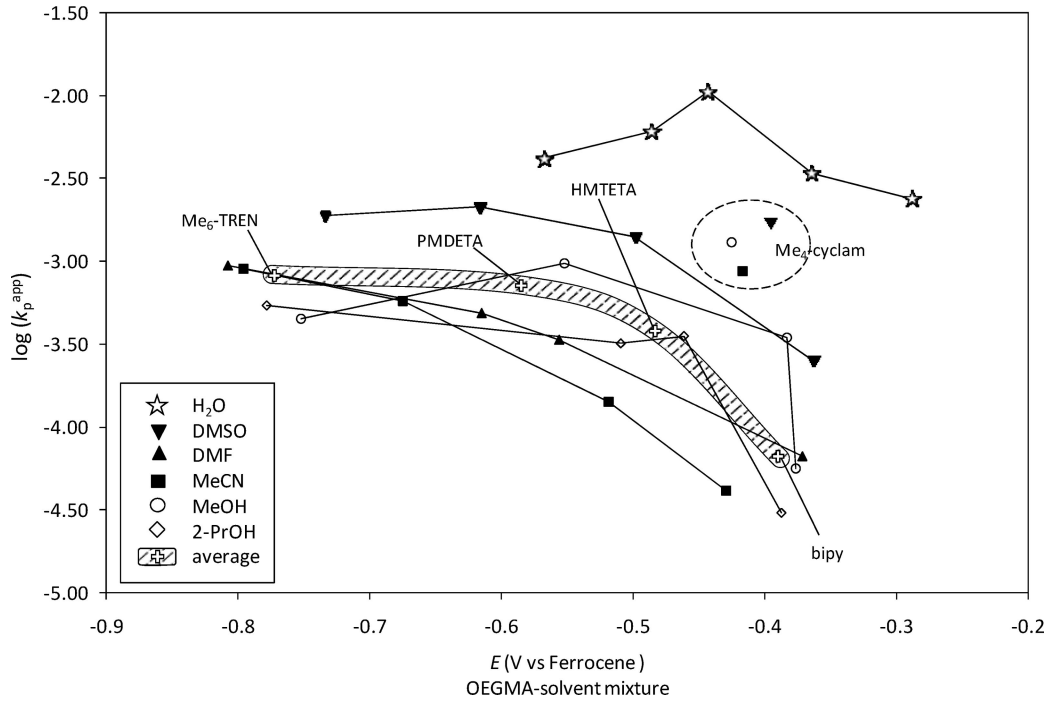

Figure 2. The logarithm of the apparent rate constant vs the half-wave potentials for various copper complexes in OEGMA−solvent mixtures, including average log(k_p^{app}) vs average E_{mix} for each complex.

$$\text{R-X} + \text{Cu(I)X/L} \leftrightarrows \text{R}^\bullet + \text{X-Cu(II)X/L} \quad \text{(a)}$$

$$\text{Cu(I)X/L} \leftrightarrows \text{Cu(II)X/L}^+ + \text{e}^- \quad \text{(b)}$$

$$\text{R-X} + \text{e}^- \leftrightarrows \text{R}^\bullet + \text{X}^- \quad \text{(c)}$$

$$\text{X}^- + \text{Cu(II)X/L}^+ \leftrightarrows \text{X-Cu(II)X/L} \quad \text{(d)}$$

Figure 3. Elementary processes of the ATRP equilibrium (a): the oxidation of the copper complex (b), the reduction of the alkyl halide (c), and the complexation of X−Cu(II)X/L (d).

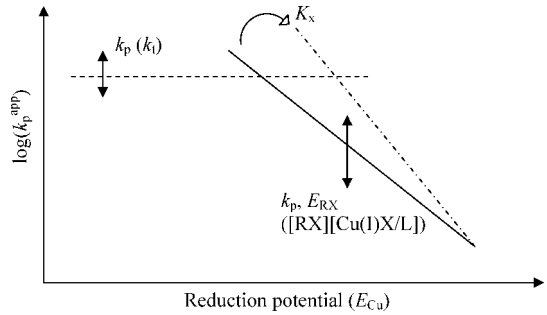

Figure 4. Straight line described by eq 5 or 6 (solid line). The horizontal dotted line represents the limit at which the apparent rate constant becomes independent of the potential.

Me$_4$-cyclam stands out from the rest of the complexes with high apparent rate constants at relatively high potentials in the nonaqueous solvents. Me$_4$-cyclam is a cyclic, more rigid ligand compared to the other ligands investigated. Oxidation of the copper complex requires reorganization of the coordination sphere, which can explain why the potentials are relatively high when the ligand is more rigid. However, the high k_p^{app} compared to, e.g., bipy, could indicate that the activation proceeds through a different mechanism compared to the other complexes, e.g. electron-transfer vs atom-transfer. This is supported by the observation that Me$_4$-cyclam fits the general trend in water.[8] In water, a different ATRP mechanism can be expected, having more the character of electron-transfer than of atom-transfer, due to dissociation of the deactivator (i.e., low halidophilicity, *vide infra*).

Table 2. Properties of the Polymerizations for the Different Copper Complex/Solvent−Mixture Combinations, and Assessment of Control over the Polymerization[a]

	H$_2$O				DMSO			
	kinetics	M_n	PDI	control	kinetics	M_n	PDI	control
Me$_6$-TREN	o	−	(−)	−	−	−	(o)	o
PMDETA	o	+	(−)	−	o	+	−	(−)
bipy	(+)	(o)	(−)	o	+	(o)	o	(+)
	2-PrOH				MeCN			
	kinetics	M_n	PDI	control	kinetics	M_n	PDI	control
Me$_6$-TREN	+	o	(o)	o	−	−	o	−
PMDETA	o	o	o	+	o	o	o	(+)
bipy	+	o	+	+	+	+	+	++

[a] Key: −, curvature in kinetics/nonlinear increase in M_n/increasing PDI values/poor control; ○, weak curvature in kinetics/linearly increasing $M_n < M_{n,th}$/low PDI values, increasing; +, first order kinetics/linearly increasing $M_n = M_{n,th}$/low PDI values/good control; ( ), properties slightly inferior to criterion (e.g., (−) = high PDI values).

From Figure 2, it is obvious that below a certain potential, the apparent rate constant is practically independent of the potential. The rationale for this is that the increased equilibrium concentration of radicals, caused by the shift in equilibrium constant, is counteracted by terminations and a build-up of the deactivator concentration (i.e., Cu^{II} species). This is also known as the persistent radical effect (PRE).[27] The kinetics of the system becomes, in a sense, self-regulating.

A general description of the limits of control for ATRP can be derived from eq 1 for the apparent rate constant

$$k_p^{app} = k_p[\text{R}^\bullet] \quad (1)$$

where k_p is the propagation rate constant for the addition of the active species (R$^\bullet$) to the double bond of the monomer (Scheme 1) and [R$^\bullet$] is the radical concentration. The radical concentration depends on the copper complex and alkyl halide reduction potentials, through the ATRP equilibrium constant (eq 2),

$$K_{ATRP} = K_a = \frac{[Cu(II)][R^\bullet]}{[Cu(I)][RX]} = K_b K_c K_d = f(E_{Cu}, E_{RX}, K_x) \quad (2)$$

where K_i are the equilibrium constants for the elementary processes of the ATRP equilibrium (Figure 3).

On the basis of the expressions for the equilibrium constants for processes b−d (Figure 3), two expressions for the radical concentration [R•] can be derived (assuming that radical−radical reactions are negligible and $[R^\bullet] = [Cu(II)]_{tot}$, detailed derivations are found in Supporting Information).[8] In solvents where K_d (also termed halidophilicity, K_x) is small (e.g., in water, $K_{Br} = 12\ M^{-1}$ for CuBr/bipy[28]), equilibrium d can be assumed to be insignificant[8] and [R•] is given by eq 3.

$$\log[R^\bullet] = \frac{1}{3}(\log K_b + \log K_c + \log([RX][Cu(I)X/L])) = \frac{1}{3}\log\left(\exp\left(\frac{F}{RT}(E_{RX} - E_{Cu})\right)[RX][Cu(I)X/L]\right) \quad (3)$$

However, in solvents where equilibrium d is significant (e.g., nonpolar organic solvents), [R•] is given by eq 4.

$$\log[R^\bullet] = \frac{1}{2}(\log K_b + \log K_c + \log K_d + \log([RX][Cu(I)X/L])) \quad (4)$$

Substituting eq 3 into eq 1, the apparent rate constant can be expressed according to eq 5. Similarly, eq 4 can be substituted into eq 1, resulting in eq 6.

$$\log(k_p^{app}) = \underbrace{\left(-\frac{1}{3}\frac{F}{RT}\frac{1}{2.3}\right)}_{\text{slope}} E_{Cu} + \underbrace{\left\{\left(\frac{1}{3}\frac{F}{RT}\frac{1}{2.3}\right)E_{RX} + \frac{1}{3}\log([RX][Cu(I)X/L]) + \log(k_p)\right\}}_{\text{intercept}} \quad (5)$$

$$\log(k_p^{app}) = \left(-\frac{1}{2}\frac{F}{RT}\frac{1}{2.3}\right)E_{Cu} + \left\{\left(\frac{1}{2}\frac{F}{RT}\frac{1}{2.3}\right)E_{RX} + \frac{1}{2}\log([RX][Cu(I)X/L]) + \frac{1}{2}\log(K_d) + \log(k_p)\right\} \quad (6)$$

Equation 5 describes a straight line in the $\log(k_p^{app})$ vs E_{Cu} plot (Figure 4) with a theoretical slope, $s_1 = -5.64$.[8] Equation 6 describes a straight line with a theoretical slope (assuming K_d to be independent of E_{Cu}):[29]

$$s_2 = -\frac{1}{2}\frac{F}{RT}\frac{1}{2.3} = -8.47$$

Although the assumption was made for these derivations that no radical−radical reactions take place, which is unlikely for any radical polymerization system, the experimental data are reasonably well described by eqs 5 and 6. The slope for the potential dependent part of the average experimental series in Figure 2, excluding the part where $s = 0$, is close to s_2 (−8.1). The slope for the OEGMA−water mixtures[8] is close to s_1 (−6.6).

At a given [RX]/[Cu(I)] ratio, the position of the line from eq 5 or 6 (i.e., the intercept) depends on system specific parameters such as the propagation rate constant (k_p), the redox properties of the alkyl halide (E_{RX}) and the halidophilicity (K_x). The apparent rate constant increases with decreasing potential, in accordance with eq 5 or 6, but at a certain point, a limit is reached where after $\log(k_p^{app})$ becomes practically independent of the potential (Figure 4). As the potential decreases further from this point, the apparent rate constant is no longer described by eq 5 or 6. The apparent rate constant at potentials below this point will be lower than the theoretical apparent rate constant, given by eq 5 and 6 (for any potential) due to the persistent radical effect (PRE)[27] (*vide supra*). The limiting value of the apparent rate constant depends on the rate constants for the radical propagation and termination reactions (k_p and k_t, respectively, Scheme 1). Increased k_p to k_t ratio raises the limit, since higher apparent rate constants can be reached at lower radical concentration (eq 1), thus suppressing the persistent radical effect. At the point where the apparent rate constant becomes independent of the potential, the ATRP process runs out of control. The choice of monomer is therefore essential for the design of an ATRP-system. The degree of control over the polymerization is dependent on the radical concentration and therefore directly related to the limiting apparent rate constant.

The solvent effect on the apparent rate constant is a combination of the solvent effects on k_p, E_{Cu}, E_{RX}, and K_x. The solvent effects on E_{RX} affect the position of the line from eq 5 and 6 (i.e., the intercept), while the solvent effects on k_p affect the position of the limiting apparent rate constant as well as the intercept. Solvent effects on K_x affect the intercept and to some extent the slope of the line ($s_2/s_1 = 1.5$). The halidophilicity is more affected by the solvent than by the complex.[29]

As illustrated in Figure 2, the solvent effects influence the potential at which k_p^{app} becomes independent of the potential and results, in general, in higher apparent rate constants in more polar solvents. This can be attributed to the solvent effects mentioned above. The effect of the solvent polarity on the propagation rate constant for various monomers has been investigated, but the results are not unambiguous. However, the propagation rate constant for MMA in various solvents (e.g., DMSO and bromobenzene) has been found to increase with increasing polarity of the solvent.[30] The slopes of the potential dependent parts in Figure 2 vary somewhat between the solvents, which can be the effect of e.g. different halidophilicities in different solvents.

The magnitude of the solvent effect on the kinetics for each complex was found to be larger than would be expected solely from the solvent effects on the potentials. The theoretical slopes of the $\log(k_p^{app})$ vs E plot (s_1 and s_2, *vide supra*) indicate a factor 4−7 increase in k_p^{app} for each 100 mV decrease in potential. However, for some of the complexes, k_p^{app} varies by more than 1 order of magnitude for a 100 mV change in potential.

Table 3. Summary of the Chain Extension Experiments

	original system [chain ext. system]	characteristics of the macroinitiator synthesis	results chain extension: reaction time (h)	results chain extension: SEC results
A	Bipy/2-PrOH [same]	low PDI value (1.22) linearly increasing M_n ($<M_{n,th}$)	47	*Figure5*
B	PMDETA/DMSO [same]	increasing PDI-value (1.58) linearly increasing M_n ($\sim M_{n,th}$)	18	*Figure5*
C	Me_6-TREN/DMSO [Bipy/DMSO]	nonlinear M_n increase ($>M_{n,th}$) low PDI value (1.23) (stopped at low conversion)	15	*Figure5*

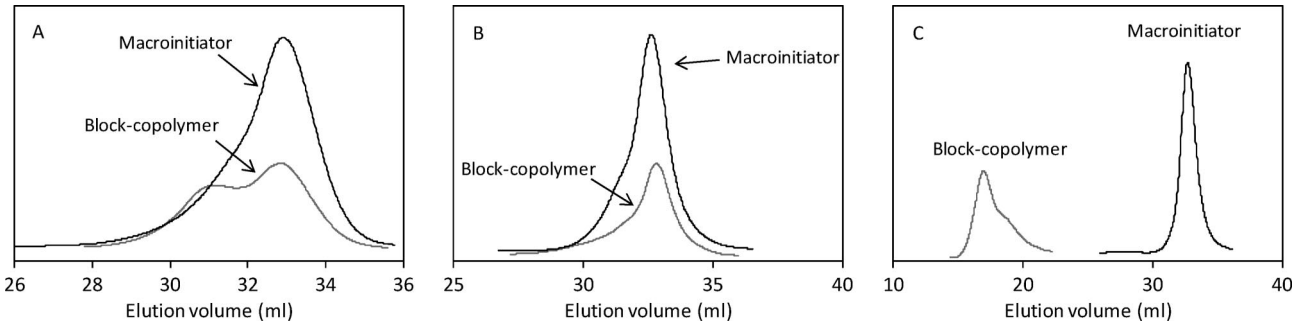

Figure 5. SEC chromatograms of macroinitiators p(OEGMA)−Br and block copolymers p(OEGMA)-*b*-p(OEGMA), for systems A, B, and C in Table 3.

The solvent effects on the apparent rate constants were also analyzed in terms of Kamlet−Taft relationships, similarly to the redox properties (Supporting Information). The relative importance of the Kamlet−Taft parameters were calculated (Table S6, Supporting Information). There is a shift in the relative importance of the parameters between the redox properties of the copper complexes and the apparent rate constants. For $\log(k_p^{app})$, the same two parameters dominate for all ligands. The rationale for this is most probably that the solvent effects on the propagation rate constant and on the alkyl halide redox properties have higher impact on the apparent rate constant than the solvent effects on the redox properties.

Polymerizations: Degree of Control and Livingness. The solvent effects on ATRP of OEGMA cannot be investigated only by examining the redox properties and apparent rate constants, since the degree of control over the polymerization and the livingness of the chain ends are essential in ATRP. The degree of control over the polymerizations was assessed by evaluating the kinetics and the molecular weights and PDI values (measured by SEC calibrated with linear PEG standards) for the different experiments (Supporting Information and Table 2). A well controlled system is defined by having first order kinetics, linearly increasing molecular weights with conversion and low PDI values. Several of the polymerization reactions were fast, with 80% conversion within two hours, and the polymerization solutions changed color immediately after addition of the initiator, indicating fast formation of Cu^{II} species. Curvature was observed in some of the kinetic plots (i.e., $\log(k_p^{app})$ vs time), indicating a significant degree of termination reactions and, hence, poor control. Several of the polymers had molecular weights increasing linearly with conversion, but being lower than the theoretical molecular weight, which could indicate e.g. chain transfer reactions. On the other hand, these polymers also exhibited relatively low PDI values, generally less than or close to 1.2. The OEGMA polymer has a brush-like structure due to the ethylene glycol side chains, giving one branch per repeating unit. It is therefore likely that the molecular weights of the synthesized OEGMA polymers are underestimated, since the calibration is performed with linear poly(ethylene oxide) samples[31] (a behavior also seen in ref 32). It was therefore concluded that low PDI values and linearly increasing molecular weights indicated good control (together with first order kinetics). In water, the polymerization rates are high and the control is poor, with high PDI values. In the other solvents, better control is generally achieved in the systems with the lowest apparent rate constants, which is also where first order kinetics, linearly increasing molecular weights and low PDI values are found. The best control is achieved with bipy, whereas Me_6-TREN, with the highest rate constants, results in poorly controlled polymerizations with high PDI values.

The degree of control and the livingness were also evaluated by attempts to perform chain extension from some of the OEGMA polymers. Three polymer samples were chosen as macroinitiators, covering a representative range of behavior during polymerization (low/high PDI values, linear/nonlinear increase of M_n, Table 3). Increasing molecular weights were observed with two of the macroinitiators, A and C (Figure 5), indicating some livingness. In system B, the extent of chain extension was negligible (Figure 5), indicating that the increasing PDI values and weakly bimodal SEC traces for the macroinitiator were due to terminations. It is difficult to draw any conclusions regarding the degree of control from these chain extension experiments. The livingness of system A seems to be poor, although the PDI values were low for the macroinitiator. However, this can be due to other factors, such as undetected side reactions during workup.

Limit of Control. From the examination of the degree of control over the polymerizations and the $\log(k_p^{app})$ vs E plot (Figure 2), an approximate limit for k_p^{app} for controlled ATRP (of OEGMA) can be estimated. The linear increase in apparent rate constant with decreasing potential levels off at $k_p^{app} \sim 7 \times 10^{-4}$ s^{-1} (for the average series), which also seems to be the limit around which the control is significantly deteriorated. It is difficult to judge whether this is a general rule applicable also to other systems. Many apparent rate constants for well controlled polymerizations in the literature are lower than 7×10^{-4} s^{-1}, which includes monomers such as styrene[33,34] and methyl acrylate[4] and ligands such as Me_6-TREN[35,36] and 4,4′-di-(5-nonyl)-2,2′-bipyridine (dNbpy).[33,34] However, *N*-isopropylacrylamide (NIPAAM) has been polymerized through ATRP in DMF/water (50/50 v/v), with CuCl/Me_6-TREN as catalyst, in a controlled manner with $k_p^{app} = 1.2 \times 10^{-3}$ s^{-1}.[17] As mentioned above, well controlled ATRP with high apparent rate constants suggests high propagation rate constants (k_p). The propagation rate constant for free radical polymerization of styrene[37] in bulk at 90 °C is 815 L mol^{-1} s^{-1} and 1504 L mol^{-1} s^{-1} for MMA[37] in bulk at 90 °C, whereas for NIPAAM[38] in water at temperatures ≤20 °C, k_p exceeds $\sim 10^4$ L mol^{-1} s^{-1}. Although the propagation rate constant for NIPAAM in the solvent mixture DMF/water is not known, these values indicate much higher propagation rate constants for NIPAAM compared to e.g. styrene. The calculated radical concentration (eq 1, assuming $k_p = 10\,000$ L mol^{-1} s^{-1}) is 1.2×10^{-7} M for NIPAAM. This value is close to reported radical concentrations for well controlled ATRP (10^{-8}−10^{-7} M),[4,33,39] confirming that low radical concentrations are essential to achieve well controlled ATRP. It also explains the high level of control for NIPAAM despite the high apparent rate constant, confirming that the apparent rate constant alone cannot be used to evaluate the level of control over an ATRP process. It is also obvious that the limit of control is system dependent (particularly depending on the monomer).

Acknowledgment. The Carl Trygger Foundation and the Swedish Research Council are acknowledged for financial support.

Supporting Information Available: Details regarding the Kamlet−Taft analyses, including tables with Kamlet Taft coefficients and relative importance of parameters. Detailed derivation of the expressions for the radical concentration. Tables with ΔE_p values. Plots of E_{mix} vs E_{pure} and of $\log(k_p^{app})$ vs E_{mix}, with the complexes in the legends. Plots of $\ln([M]_0/[M])$ vs time and molecular weights and PDI values for the polymerizations. This information is available free of charge via the Internet at http://pubs.acs.org.

References and Notes

(1) Kato, M.; Kamigaito, M.; Sawamoto, M.; Higashimura, T. *Macromolecules* **1995**, *28*, 1721–1723.
(2) Wang, J.-S.; Matyjaszewski, K. *J. Am. Chem. Soc.* **1995**, *117*, 5614–5615.
(3) Xia, J.; Matyjaszewski, K. *Macromolecules* **1997**, *30*, 7697–7700.
(4) Wang, J.-S.; Matyjaszewski, K. *Macromolecules* **1995**, *28*, 7901–7910.
(5) Xia, J.; Gaynor, S. G.; Matyjaszewski, K. *Macromolecules* **1998**, *31*, 5958–5959.
(6) Matyjaszewski, K.; Gobelt, B.; Paik, H.-j.; Horwitz, C. P. *Macromolecules* **2001**, *34*, 430–440.
(7) Qiu, J.; Matyjaszewski, K.; Thouin, L.; Amatore, C. *Macromol. Chem. Phys.* **2000**, *201*, 1625–1631.
(8) Coullerez, G.; Carlmark, A.; Malmström, E.; Jonsson, M. *J. Phys. Chem. A.* **2004**, *108*, 7129–7131.
(9) Coullerez, G.; Malmström, E.; Jonsson, M. *J. Phys. Chem. A.* **2006**, *110*, 10355–10360.
(10) Matyjaszewski, K.; Wei, M.; Xia, J.; McDermott, N. E. *Macromolecules* **1997**, *30*, 8161–8164.
(11) Kajiwara, A.; Matyjaszewski, K. *Macromolecules* **1998**, *31*, 5695–5701.
(12) Xia, J.; Zhang, X.; Matyjaszewski, K. *Macromolecules* **1999**, *32*, 3531–3533.
(13) Coca, S.; Jasieczek, C. B.; Beers, K. L.; Matyjaszewski, K. *J. Polym. Sci., Part A: Polym. Chem.* **1998**, *36*, 1417–1424.
(14) Wang, X.-S.; Lascelles, S. F.; Jackson, R. A.; Armes, S. P. *Chem. Commun.* **1999**, *181*, 7–1818.
(15) Matyjaszewski, K.; Nakagawa, Y.; Jasieczek, C. B. *Macromolecules* **1998**, *31*, 1535–1541.
(16) Masci, G.; Bontempo, D.; Tiso, N.; Diociaiuti, M.; Mannina, L.; Capitani, D.; Crescenzi, V. *Macromolecules* **2004**, *37*, 4464–4473.
(17) Masci, G.; Giacomelli, L.; Crescenzi, V. *Macromol. Rapid Commun.* **2004**, *25*, 559–564.
(18) Iddon, P. D.; Robinson, K. L.; Armes, S. P. *Polymer* **2004**, *45*, 759–768.
(19) Nanda, A. K.; Matyjaszewski, K. *Macromolecules* **2003**, *36*, 599–604.
(20) Nanda, A. K.; Matyjaszewski, K. *Macromolecules* **2003**, *36*, 1487–1493.
(21) Matyjaszewski, K.; Paik, H.-j.; Zhou, P.; Diamanti, S. J. *Macromolecules* **2001**, *34*, 5125–5131.
(22) Chung, H.; Tang, W.; Matyjaszewski, K. *Polym. Prepr. (Am. Chem. Soc., Div. Polym. Chem.)* **2008**, *49*, 97–98.
(23) Braunecker, W. A.; Tsarevsky, N. V.; Gennaro, A.; Matyjaszewski, K. *Polym. Prepr. (Am. Chem. Soc., Div. Polym. Chem.)* **2008**, *49*, 376–377.
(24) Wang, X.-S.; Armes, S. P. *Macromolecules* **2000**, *33*, 6640–6647.
(25) Ciampolini, M.; Nardi, N. *Inorg. Chem.* **1966**, *5*, 41–44.
(26) Hammerich, O. In *Organic Electrochemistry*, 4th ed.; Lund, H., Hammerich, O., Eds.; Marcel Dekker: New York, 2001; pp 95−182.
(27) Fischer, H. *Chem. Rev.* **2001**, *101*, 3581–3610.
(28) Pintauer, T.; McKenzie, B.; Matyjaszewski, K. *Polym. Prepr. (Am. Chem. Soc., Div. Polym. Chem.)* **2002**, *43*, 217–218.
(29) The variation in K_{Br} between different solvents is larger than between different copper complexes.[28] Since E_{Cu} was found to vary more between copper complexes than between solvents (present work), it can be assumed that K_d is independent of E_{Cu}. ΔK_{Br} (solvents) > ΔK_{Br} (ligands). ΔE_{Cu} (solvents) < ΔE_{Cu} (ligands)
(30) Zammit, M. D.; Davis, T. P.; Willett, G. D.; O'Driscoll, K. F. *J. Polym. Sci., Part A: Polym. Chem.* **1997**, *35*, 2311–2321.
(31) Branched polymers have lower hydrodynamic volumes than linear polymers of the same molecular weight, which can, when SEC calibration is performed with linear polymers, be interpreted as lower than expected molecular weights.
(32) Lutz, J.-F.; Hoth, A. *Macromolecules* **2006**, *39*, 893–896.
(33) Matyjaszewski, K.; Patten, T. E.; Xia, J. *J. Am. Chem. Soc.* **1997**, *119*, 674–680.
(34) Kajiwara, A.; Matyjaszewski, K. *Macromolecules* **1998**, *31*, 5695–5701.
(35) Queffelec, J.; Gaynor, S. G.; Matyjaszewski, K. *Macromolecules* **2000**, *33*, 8629–8639.
(36) Inoue, Y.; Matyjaszewski, K. *Macromolecules* **2004**, *37*, 4014–4021.
(37) Hutchinson, R. A.; Aronson, M. T.; Richards, J. R. *Macromolecules* **1993**, *26*, 6410–6415.
(38) Ganachaud, F.; Balic, R.; Monteiro, M. J.; Gilbert, R. G. *Macromolecules* **2000**, *33*, 8589–8596.
(39) Wang, J.-L.; Grimaud, T.; Matyjaszewski, K. *Macromolecules* **1997**, *30*, 6507–6512.

MA8028425